Model Predictive Control of Urban Drainage Systems Considering Uncertainty

Jan Lorenz Svensen, Congcong Sun, Gabriela Cembrano and Vicenç Puig

***Abstract*— This brief contributes to the application of model predictive control (MPC) to address the combined sewer overflow (CSO) problem in urban drainage systems (UDSs) with uncertainty. In UDS, dealing with uncertainty in rain forecast and dynamic models is crucial due to the possible impact on the UDS control performance. Two different MPC approaches are considered: tube-based MPC (T-MPC) and chance-constrained MPC (CC-MPC), which represent uncertainty in deterministic and stochastic manners, respectively. This brief presents how to apply T-MPC to UDS, by establishing a mathematical relation with CC-MPC, and a rigorous mathematical comparison. Based on simulations using the Astlingen benchmark UDS, the strengths and weaknesses of the performance of T-MPC and CC-MPC in UDS were compared. Differences in the involved mathematical computations have also been analyzed. Moreover, the comparison in performance also indicates the applicability of each MPC approach in different uncertainty scenarios.**

***Index Terms*— Chance-constrained, combined sewer overflow (CSO), model predictive control (MPC), tube, uncertainty, urban drainage system (UDS).**

I. Introduction

URBAN drainage systems (UDSs) are critical infrastructures that transport wastewater and rainwater to be treated in wastewater treatment plants (WWTPs) before releasing them into the environment. However, in heavy-rain situations, the water inflow may exceed infrastructure capacity, causing overflows and pollution to the recipient environment, which is the combined sewer overflow (CSO). Therefore, one important operational objective of UDS is to reduce the pollution of CSO. Model predictive control (MPC) has been proven an adequate approach in practice and research for such objectives [1], [2], [3], [4].

MPC is an optimal control method, which has been matured into a well-researched field and an effective approach to solve multivariable constrained control problems in many types of infrastructures; water networks, smart grids, etc., [1], [2], [3], [5], [6], [7], [8], [9], [10], [11], [12], [13], [14], [15], [16], [17], [18]. For the UDS application, the majority of MPC research has focused on the case with deterministic rain forecasts, with only a few having considered the uncertainties [17], [18]. However, in reality, the dynamic models and rainfall forecasts would include uncertainties possibly affecting the operation of UDS, which might involve more CSO and the consequent pollution of the environment [19].

Handling uncertainty is, therefore, important within MPC [5], [6], [8], [16], [17], [18], [20], [21], [22], [23], [24], [25], [26], [27], [28], [29]. Depending on whether uncertainty models are deterministic or statistic, the MPC extensions can be grouped into robust or stochastic methods. In [17] and [18], the presence of CSO complicates the handling of uncertainties in UDS using stochastic chance-constrained MPC (CC-MPC), with the need for a weir-oriented reformulation.

Therefore, this brief will consider and verify how a robust approach: tube-based MPC (T-MPC) using zonotopes, can be applied to the case of UDS with uncertainty, both in theory and application in comparison to CC-MPC. This brief contributes:

1) a formulation of the zonotopic T-MPC applicable to UDS with uncertainties;
2) a mathematical comparison of T-MPC and CC-MPC, their constraint formulations, and the propagation of uncertainty;
3) a performance comparison of T-MPC and CC-MPC in solving the CSO problem in UDS, based on a well-known benchmark the Astlingen UDS; and
4) a comparative discussion to clarify selections of MPC approaches.

A. Related Work

Robust MPCs use set knowledge to bound uncertainties, considering the worst case of the constraints and occasionally cost function [8], [16], [21], [24], [27], [29]. The easiest way relies on exploiting inherent robustness, where open-loop control action is determined without explicitly considering uncertainties [19]. However, due to the possible diminished control performance, feedback control could be designed to explicitly consider uncertainty [27], [29]. For robust MPC, the min–max approach is a common method, which leads to conservative results [26] and generally intractable computational load [16]. T-MPC is the robust approach with conservative solutions at reasonable computational loads [8], [24], [30], which bounds the uncertainty deviation through a sequence of invariant sets in the state space, the so-called tubes [6], [21], [25].

Stochastic MPC considers the probabilistic nature of uncertainties in the controller design [28] through using a stochastic distribution of the uncertainty to ensure that the control strategies satisfy the constraints for the most likely realizations [5],

Manuscript received 25 April 2023; accepted 9 June 2023. Date of publication 3 July 2023; date of current version 23 October 2023. This work was supported in part by the Supervision and fault-tolerant control of smart infrastructures based on advanced learning and optimization (L-BEST) Project of the Spanish Agency of Research under Grant PID2020-115905RB-C21 and in part by the Real-time pollution-based control of urban drainage and sanitation systems for protection of receiving waters (RUBIES) Project of the European Commission under Grant LIFE20 ENV/FR/000179. Recommended by Associate Editor G. Papafotiou. *(Corresponding author: Jan Lorenz Svensen.)*

Jan Lorenz Svensen is with the Department of Applied Mathematics and Computer Science, Technical University of Denmark, 2800 Kongens Lyngby, Denmark (e-mail: jlsv@dtu.dk).

Congcong Sun is with the Agricultural Biosystems Engineering Group, Wageningen University, 6700 AA Wageningen, The Netherlands (e-mail: congcong.sun@wur.nl).

Gabriela Cembrano and Vicenç Puig are with the Control Systems Group, Institut de Robòtica i Informàtica Industrial (CSICUPC), 08028 Barcelona, Spain (e-mail: gcembrano@iri.upc.edu; vpuig@iri.upc.edu).

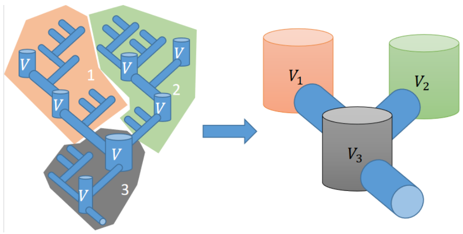

Fig. 1. Modeling concept for virtual tanks.

[20], [22], [23], [25], [28], [31], [32]. Stochastic MPC includes approaches from scenario-based MPC [31] to CC-MPC [33].

The CC-MPC method uses probabilistic constraints considering the violation probability under a chosen confidence level [34], with application in several domains [5], [18], [20], [22]. The scenario-based MPC approximates the robust approach, and is a simple method, though its pure form scales badly for high probabilistic coverage, the linear case is scalable for approximating CC-MPC [35]. Both methods have been applied and compared in water network management [36].

Although T-MPC and CC-MPC are typical representative approaches in the robust and stochastic families of MPC, there has been no comparison between them especially in the UDS application. The selection of the two approaches T-MPC and CC-MPC comes from the facts that: 1) they have a similar approach to constraints, both relying on tightening, and 2) they resemble each other from the mathematical perspective.

B. Nomenclature

In this brief, vectors and matrices are denoted by bold font, and the dimension of a function or variable $\mathbf{f}$ is given by n_f. The minimum and maximum of a function $f(x)$ are noted by $\underline{f}$ and $\overline{f}$, respectively, while the sampling time and sample number are denoted by ΔT and the subscript k, respectively. A stochastic variable X following a distribution F is written as $X \sim F$, while its expectation is given by $E\{X\}$. The probability function for the value of x is denoted by $\Pr\{X \leq x\}$, likewise, the cumulative distribution function (cdf) is given by $\Phi_X\{x\}$.

II. MPC Design for UDS

A. Control-Oriented Model

The control model in this brief is based on [37], where the UDS was divided into connected subgroups of catchments and treated as interconnected *virtual tanks*, see Fig. 1. The model for catchments or virtual tanks at the kth time step was based on the water volume balance

$$\mathbf{v}_{k+1} = \mathbf{v}_k + \Delta T(\mathbf{q}_k^{\text{in}} - \mathbf{q}_k^{\text{out}} - \mathbf{q}_k^{\text{CSO}}) \tag{1}$$

where $\mathbf{v}_k$ is water volume of catchments or tanks at time step k; ΔT is the time interval; and $\mathbf{q}_k^{\text{in}}$, $\mathbf{q}_k^{\text{out}}$, and $\mathbf{q}_k^{\text{CSO}}$ are sum of inflows, outflows, and the amount of overflow, respectively.

The tanks are connected with main sewage pipes which convey outflows from tanks $\mathcal{T}$ and inflows from the environment

$$q_{i,k}^{\text{in}} = q_{i,k}^{\text{house}} + \varphi_i S_i P_{i,k} + \sum_{j \in \mathcal{T}} q_{j,k-d_j}^{\text{out}} \tag{2}$$

where q_i^{house} is the wastewater from houses, φ_i is the ground absorption coefficient, S_i is the area, and $P_{i,k}$ is the precipitation intensity in ΔT for the ith catchment, with d_j being the delay time of the outflows through the pipe. The outflows are either passive or controlled. Passive outflows are assumed to be proportional to the tank level

$$q_{i,k}^{\text{out}} = \beta_i v_{i,k} \tag{3}$$

where calibration procedure of φ and β is given by [38]. In the controlled case, the tank outflow is controlled directly through the variables u_i using a *retention gate*, $q_{i,k}^{\text{out}} = u_{i,k}$. While pipes use *redirection gates* to divert flow from the outflow

$$q_{i,k}^{\text{out}} = q_{i,k}^{\text{in}} - \sum_j u_{i,k}^j \tag{4}$$

where j is the index of manipulated flows. Based on the presented models, the collected tank volumes of UDS is

$$\mathbf{x}_{k+1} = \mathbf{A}\mathbf{x}_k + \mathbf{B}\mathbf{u}_k + \mathbf{B}_{\text{cso}}\mathbf{q}_k^{\text{CSO}} + \mathbf{G}\mathbf{w}_k \tag{5}$$

where $\mathbf{x}_k$ is a vector with states such as tank volumes, $\mathbf{u}_k$ represents manipulated flows, $\mathbf{w}_k$ corresponds to rain and wastewater inflows, $\mathbf{q}_k^{\text{CSO}}$ represents the overflows, and constant matrices $\mathbf{A}$, $\mathbf{B}$, $\mathbf{B}_{\text{cso}}$, and $\mathbf{G}$ are the system matrices.

B. Model Constraints

For MPC in UDS, the constraints typically describe the limits of the different flows in the network (e.g., $q_{i,k}^{\text{out}} \leq \bar{q}_i^{\text{out}}$), or the limits on tank volumes [18], [39]. The complete set of constraints can usually be written as

$$\boldsymbol{\Psi}\mathbf{x}_k + \boldsymbol{\Gamma}\mathbf{u}_k + \boldsymbol{\Gamma}_{\text{cso}}\mathbf{q}_k^{\text{CSO}} + \boldsymbol{\Theta}\mathbf{w}_k \leq \boldsymbol{\phi}. \tag{6}$$

C. Control Objectives

Control of UDS may have multiple objectives [4] with decreasing priority order: Objective 1) minimization of CSO volume; Objective 2) maximizing flow to the WWTP; and Objective 3) minimizing control changes.

The overflows in the first objective can be described either through logic ($q_{j,k}^{\text{CSO}} = 0 \leftrightarrow v_{j,k} \leq \bar{v}_j$) or slack variables

$$\text{rcl}(v_{j,k} - \overline{v}_j)/\Delta T \leq q_{j,k}^{\text{CSO}}, \qquad 0 \leq q_{j,k}^{\text{CSO}}. \tag{7}$$

Typically, the above objectives are formulated using norms

$$\text{cccl}_1 = \|\boldsymbol{\Xi}_{\text{cso}}\|_1 \quad l_2 = -\|\boldsymbol{\Xi}_{\text{TP}}\|_1 \quad l_3 = \|\boldsymbol{\Xi}_{\Delta u}\|_2 \tag{8}$$

where $\boldsymbol{\Xi}_{\text{cso}}$ is a weighted vector containing the CSO volume across the prediction horizon H_p. Similarly, $\boldsymbol{\Xi}_{\text{TP}}$ contains the flows to the WWTPs, and $\boldsymbol{\Xi}_{\Delta u}$ contains the changes of control actions. Other objectives or priorities can exist.

For both overflow and wastewater treatment, the 1-norm is used to optimize the total quantity and not specific peaks.

III. MPC Methods: Tube and Chance Constrained

In this section, we outline and compare the MPC methods used in this brief. A detailed focus will be given to the case of linear systems with additive uncertainty, as it is a standard approach to represent UDS, using virtual tanks [39]. If we denote a sequence of states, inputs, and disturbances, respectively, by

$$\mathbf{X}_{i|k} = [\mathbf{x}_{0|k}^T \quad \mathbf{x}_{1|k}^T \quad \dots \quad \mathbf{x}_{i|k}^T]^T \tag{9}$$

$$\mathbf{U}_{i|k} = [\mathbf{u}_{0|k}^T \quad \mathbf{u}_{1|k}^T \quad \dots \quad \mathbf{u}_{i|k}^T]^T \tag{10}$$
$$\mathbf{W}_{i|k} = [\mathbf{w}_{0|k}^T \quad \mathbf{w}_{1|k}^T \quad \dots \quad \mathbf{w}_{i|k}^T]^T \tag{11}$$

then, the general deterministic MPC with a prediction horizon H_p, minimizing a cost l subject to the constraints of a process function: $\mathbf{f} : \mathbb{R}^{n_x+n_u+n_w} \to \mathbb{R}^{n_x}$, and an inequality constraint function: $\mathbf{g} : \mathbb{R}^{n_x+n_u+n_w} \to \mathbb{R}^{n_g}$, is given by

$$J = \min_{\mathbf{U}_{H_p-1|k}} l(\mathbf{X}_{H_p|k}, \mathbf{U}_{H_p-1|k}, \mathbf{W}_{H_p-1|k}) \tag{12}$$
$$\text{s.t.} \quad \mathbf{x}_{i+1|k} = \mathbf{f}(\mathbf{x}_{i|k}, \mathbf{u}_{i|k}, \mathbf{w}_{i|k}), \quad i = 0, \dots, H_p - 1 \tag{13}$$
$$\mathbf{g}_i(\mathbf{x}_{i|k}, \ \mathbf{u}_{i|k}, \mathbf{w}_{i|k}) \leq \bar{\mathbf{g}}_i, \quad i = 0, \dots, H_p - 1. \tag{14}$$

For the linear case, the process and jth constraint is

$$\mathbf{f}(\mathbf{x}_{i|k}, \mathbf{u}_{i|k}, \mathbf{w}_{i|k}) = \mathbf{A}\mathbf{x}_{i|k} + \mathbf{B}\mathbf{u}_{i|k} + \mathbf{G}\mathbf{w}_{i|k} \tag{15}$$
$$g_{i,j}(\mathbf{x}_{i|k}, \mathbf{u}_{i|k}, \mathbf{w}_{i|k}) = \mathbf{\Psi}_{i,j}\mathbf{x}_{i|k} + \mathbf{\Gamma}_{i,j}\mathbf{u}_{i|k} + \mathbf{\Theta}_{i,j}\mathbf{w}_{i|k} \leq \phi_{i,j} \tag{16}$$

where

$$\mathbf{A} \in \mathbb{R}^{n_x \times n_x}, \ \mathbf{B} \in \mathbb{R}^{n_x \times n_u}, \ \mathbf{G} \in \mathbb{R}^{n_x \times n_w} \tag{17}$$
$$\mathbf{\Psi}_{i,j} \in \mathbb{R}^{1 \times n_x}, \ \mathbf{\Gamma}_{i,j} \in \mathbb{R}^{1 \times n_u}, \mathbf{\Theta}_{i,j} \in \mathbb{R}^{1 \times n_w}, \ \phi_{i,j} \in \mathbb{R}. \tag{18}$$

The state at the ith time can be written as

$$\mathbf{x}_{i|k} = \mathbf{A}^i\mathbf{x}_{0|k} + \sum_{j=0}^{i-1} \mathbf{A}^{i-1-j}\mathbf{B}\mathbf{u}_{j|k} + \sum_{j=0}^{i-1} \mathbf{A}^{i-1-j}\mathbf{G}\mathbf{w}_{j|k} \tag{19}$$

describing the propagation of inputs and disturbances. The corresponding propagated jth constraint is given by

$$\mathbf{\Psi}_{i,j}\mathbf{A}^i\mathbf{x}_{0|k} + \tilde{\mathbf{\Gamma}}_{i,j}\mathbf{U}_{i|k} + \tilde{\mathbf{\Theta}}_{i,j}\mathbf{W}_{i|k} \leq \phi_{i,j} \tag{20}$$

with the new constraint matrices being

$$\tilde{\mathbf{\Theta}}_{i,j} = [\mathbf{\Psi}_{i,j}\mathbf{A}^{i-1}\mathbf{G} \quad \mathbf{\Psi}_{i,j}\mathbf{A}^{i-2}\mathbf{G} \dots \mathbf{\Psi}_{i,j}\mathbf{G} \quad \mathbf{\Theta}_{i,j}] \tag{21}$$
$$\tilde{\mathbf{\Gamma}}_{i,j} = [\mathbf{\Psi}_{i,j}\mathbf{A}^{i-1}\mathbf{B} \quad \mathbf{\Psi}_{i,j}\mathbf{A}^{i-2}\mathbf{B} \dots \mathbf{\Psi}_{i,j}\mathbf{B} \quad \mathbf{\Gamma}_{i,j}]. \tag{22}$$

T-MPC and CC-MPC are discussed in the following, for the case of uncertainty being present. In both cases, the dynamics in (13) are substituted into the cost and constraint formulations.

A. Tube-Based

Robust methods deal with uncertainty by handling the worst case scenario [25]. As this depends on knowing all values the uncertainty can take, it usually requires the uncertainty to be bounded. If each disturbance $w_{i|k}$ is bounded by $\mathcal{W}_{i|k}$, then $\mathcal{W}_i$ bounding $\mathcal{W}_{i|k}$ is a tube of temporal sets

$$\mathcal{W}_i = \mathcal{W}_{0|k} \times \mathcal{W}_{1|k} \times \dots \times \mathcal{W}_{i|k} \tag{23}$$
$$\mathcal{W}_{i|k} = \{\mathbf{w}_{i|k} : \underline{\mathbf{w}}_{i|k} \leq \mathbf{w}_{i|k} \leq \overline{\mathbf{w}}_{i|k}\} \subseteq \mathbb{R}^{n_w}. \tag{24}$$

The cost of T-MPC is typically formulated as the minimization of the nominal cost [25]. The cost is defined as the minimization using the nominal system $\tilde{\mathbf{x}}_{i+1|k} = \mathbf{f}(\tilde{\mathbf{x}}_{i|k}, \mathbf{u}_{i|k}, \tilde{\mathbf{w}}_{i|k})$

$$J = \min_{\mathbf{U}_{H_p-1|k}} l(\tilde{\mathbf{X}}_{H_p|k}, \mathbf{U}_{H_p-1|k}, \tilde{\mathbf{W}}_{H_p-1|k}). \tag{25}$$

In contrast, the constraints in T-MPC are given by maximization for the worst case scenario

$$\max_{\mathbf{W}_{i|k} \in \mathcal{W}_i} \mathbf{g}_i(\mathbf{x}_{i|k}, \mathbf{u}_{i|k}, \mathbf{w}_{i|k}) \leq \bar{\mathbf{g}}_i, \quad i = 0, \dots, H_p - 1 \tag{26}$$

maximized over $\mathbf{W}_{i|k}$ with $\mathbf{x}_{i|k}$ given by (19). The maximization of each constraint $g_{i,j}$ and cost are done independently, as different realizations can be the worst case in each one of them.

In this brief, the T-MPC is formulated using zonotopes [40]. Zonotopes of $\mathbf{W}_{i|k}$ describe the disturbances by a nominal center $\tilde{\mathbf{W}}_{i|k}$ and a symmetric 0-centered uncertainty $\Delta\mathbf{W}_{i|k}$

$$\mathbf{W}_{i|k} = \tilde{\mathbf{W}}_{i|k} + \Delta\mathbf{W}_{i|k}, \quad \Delta\mathbf{W}_{i|k} \in [-\overline{\Delta\mathbf{W}}_{i|k}, \overline{\Delta\mathbf{W}}_{i|k}] \tag{27}$$
$$\tilde{\mathbf{W}}_{i|k} = \frac{1}{2}(\overline{\mathbf{W}}_{i|k} + \underline{\mathbf{W}}_{i|k}), \quad \overline{\Delta\mathbf{W}}_{i|k} = \frac{1}{2}(\overline{\mathbf{W}}_{i|k} - \underline{\mathbf{W}}_{i|k}) \tag{28}$$

with the zonotope form of $\Delta\mathbf{W}_{i|k}$ given by

$$\Delta\mathbf{W}_{i|k} \in \mathbf{0} \oplus H_{w,i}\mathbf{z}_{d,i}, \quad \mathbf{z}_{d,i} \in [-1, 1]^{(i+1) \times n_w} \tag{29}$$
$$H_{w,i} = \text{diag}(\overline{\Delta\mathbf{w}_{0|k}}, \dots, \overline{\Delta\mathbf{w}_{i|k}}) \tag{30}$$

where $\oplus$ denotes the Minkowski sum, the $\mathbf{0}$-vector is the center of the $\Delta\mathbf{W}_{i|k}$zonotope, and $H_{w,i}\mathbf{z}_{d,i}$ is the set of boundaries.

Using zonotopes, it is easier to propagate uncertainty in the dynamics. In the linear case of the jth constraint, (20), the propagated uncertainty can be described by the zonotope $\Delta_{i,j}$

$$\Delta_{i,j} = \tilde{\mathbf{\Theta}}_{i,j}\Delta\mathbf{W}_{i|k} \in \mathbf{0} \oplus \tilde{\mathbf{\Theta}}_{i,j}H_{w,i}\mathbf{z}_{d,i}. \tag{31}$$

For the T-MPC's maximization of the constraints, the linear case using zonotopes becomes simple to compute; by obtaining the largest value using the 1-norm to compute the interval hull of the zonotopes [6]

$$\overline{\Delta_{i,j}} = \|\tilde{\mathbf{\Theta}}_{i,j}H_{w,i}\|_1 \quad i \geq 0. \tag{32}$$

The robust tightening of the constraint then gives

$$\mathbf{\Psi}_{i,j}\mathbf{A}^i\mathbf{x}_{0|k} + \tilde{\mathbf{\Gamma}}_{i,j}\mathbf{U}_{i|k} + \tilde{\mathbf{\Theta}}_{i,j}\tilde{\mathbf{W}}_{i|k} \leq \phi_{i,j} - \overline{\Delta_{i,j}}. \tag{33}$$

B. Chance-Constraint

Stochastic methods are based on the assumption that disturbances follow some known distribution F

$$\mathbf{W}_{i|k} \sim F_{\mathbf{a}}^{\mathbf{b}}(\boldsymbol{\theta}), \quad \mathbf{a} \leq \mathbf{b} \tag{34}$$

defined by the parameters $\boldsymbol{\theta}$, in the intervals between $\mathbf{a}$ and $\mathbf{b}$, potentially an open interval $(-\infty \leq a_j \leq b_j \leq \infty)$.

In CC-MPC, the optimum focuses on the expected cost

$$J = \min_{\mathbf{U}_{H_p-1|k}} \mathbb{E}\{l(\mathbf{X}_{H_p|k}, \mathbf{U}_{H_p-1|k}, \mathbf{W}_{H_p-1|k})\} \tag{35}$$

using the knowledge of the distribution to account for the most likely case [5], [25]. The constraints are formulated as probabilistic constraints with a confidence level γ

$$\Pr\{\mathbf{g}_i(\mathbf{X}_{i|k}, \mathbf{U}_{i|k}, \mathbf{W}_{i|k}) \leq \bar{\mathbf{g}}_i\} \geq \gamma_i, \ i = 0, \dots, H_p - 1 \tag{36}$$
$$\iff \Phi^{-1}_{\mathbf{g}_i(\mathbf{X}_{i|k}, \mathbf{U}_{i|k}, \mathbf{W}_{i|k})}\{\gamma_i\} \leq \bar{\mathbf{g}}_i, \quad 0 \leq \gamma_i \leq 1 \tag{37}$$

where γ_i defines how robust the constraint is, as the likelihood of (14) being true. Typically, the constraints are given in terms of their quantile function $\Phi^{-1}_{\mathbf{g}_i}\{\gamma_i\}$ as shown in (37), if it exists. In this brief, we will focus on the scalar probabilistic constraints formulation. In the vector constraint case, the joint probability confidence level can be ensured by conservative element-wise risk allocation, as described in [5].

For the linear case, the constraint in (14) can be written as

$$\mathbf{\Psi}_{i,j}\mathbf{A}^{i-1}\mathbf{x}_{0|k} + \tilde{\mathbf{\Gamma}}_{i,j}\mathbf{U}_{i|k} \leq \phi_{i,j} - \Phi^{-1}_{\tilde{\mathbf{\Theta}}_{i,j}\mathbf{W}_{i|k}}\{\gamma_{i,j}\} \tag{38}$$

making the propagated disturbance term a probabilistic tightening on the constraint [41]. Even in the linear case, computing the propagated distribution of $\tilde{\mathbf{\Theta}}_{i,j}\mathbf{W}_{i|k}$ and its quantile is only simple for special cases, such as Gaussian distributions.

C. Relation of Constraint Tightening

As the T-MPC's worst case approach considers all possibilities equally important or likely, this is equivalent to assuming $\mathbf{W}_{i|k}$ to be uniformly distributed [42] within an interval (a, b)

$$\begin{aligned} &\mathbf{W}_{i|k} \sim \mathcal{U}(\mathbf{a}, \mathbf{b}) \\ &(\mathbf{a}, \mathbf{b}) = (\tilde{\mathbf{W}}_{i|k} - \overline{\Delta\mathbf{W}}_{i|k}, \tilde{\mathbf{W}}_{i|k} + \overline{\Delta\mathbf{W}}_{i|k}). \end{aligned} \tag{39}$$

This stochastic form of the worst case leads to the relationship between the constraint tightenings, given in Theorem 1.

Theorem 1: If $\tilde{\mathbf{\Theta}}_{i,j}\mathbf{W}_{i|k}$ is upper bounded, and we consider the centered part $\tilde{\mathbf{\Theta}}_{i,j}\tilde{\mathbf{W}}_{i|k}$ of the zonotope part of the constraint tightening for the T-MPC, then the constraint tightening of T-MPC and CC-MPC is related by

$$\Phi^{-1}_{\tilde{\mathbf{\Theta}}_{i,j}\mathbf{W}_{i|k}}\{\gamma_{i,j}\} \leq \tilde{\mathbf{\Theta}}_{i,j}\tilde{\mathbf{W}}_{i|k} + \|\tilde{\mathbf{\Theta}}_{i,j}H_{w,i}\|_1 \quad \forall\gamma_{i,j} \in [0, 1]$$

with the two methods being identical at $\gamma_{i,j} = 1$.

Proof: For any upper-bounded stochastic variable X of some distribution F_a^b and confidence levels $\gamma_1 \leq \gamma_2$; the quantile of γ_1 is smaller than the quantile of γ_2. It naturally follows that a $\gamma = 1$ corresponds to the upper bound

$$X \sim F_a^b(\boldsymbol{\theta}), \quad a \leq X \leq b, \quad 0 \leq \gamma_1 \leq \gamma_2 \leq 1 \tag{40}$$

$$\Phi_X^{-1}\{\gamma_1\} \leq \Phi_X^{-1}\{\gamma_2\} \leq \Phi_X^{-1}\{1\} = b. \tag{41}$$

Since the constraint on the right-hand side of (40) corresponds to the upper bound of constraints uncertainty, the right-hand side is, therefore, equal or larger than the quantile function of any distribution for the given variable. ■

IV. Application to UDS

A. UDS Case Study System

The Astlingen UDS is a well-known case study [3], [43] including both combined and separated sewer systems as seen in Fig. 2. The system includes six storage tanks (where tanks 1 and 5 are not controlled) with a total storage volume of 5900 m^3. It also contains weir structures where CSOs may occur (CSO 1–6), located in water detentions (tanks 1–6), and diversion structures (CSO 7–10). The system includes two receiving bodies for CSO, a creek and a river, where the latter is the preferred receiver. It is also driven by the unknown rain inflow as disturbances. We will use the validated simulation setup of [3], where the MPC controller is implemented in MATLAB, a Hi-Fi simulator of the system is given in SWMM[1] with a connection to MATLAB through pySWMM Python package.

[1]U.S. EPA's Storm Water Management Model.

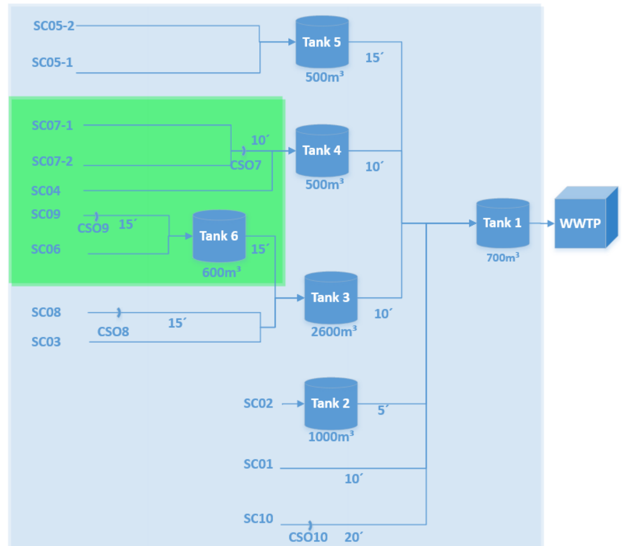

Fig. 2. Astlingen UDS [43] with interconnections between tanks, CSO pipes, WWTP, and pipe delays x' in minutes. The creek receives CSOs come from the green section and the river receives CSO from the blue section.

B. MPC Designs

The linear model of Astlingen is used to design MPC [18], where CSO flows are determined by penalty costs [2], [44], and the only uncertainties considered are in the inflow.

Since the MPC objective function formulation presented in this brief does not follow the standard formulation based on tracking a reference, the standard stability results in the literature based on terminal ingredients do not apply [9]. So, stability conditions have not been explicitly considered in the MPC designs. Formal proof of stability is considered for future research since it would require a completely new stability development. In addition, UDS' are intrinsically stable and feasible systems, as excessive water becomes CSO.

Given the different flow times between each tank, delay states are needed. Using a 5-min sampling time, the model of the UDS is discretized. The following state $\mathbf{x}_{i|k}$, manipulation $\mathbf{u}_{i|k}$, and disturbance $\mathbf{w}_{i|k}$ are considered

$$\begin{aligned} \mathbf{x}_{i|k} = [&V_{i|k}^{T1}, V_{i|k}^{T2}, V_{i|k}^{T3}, V_{i|k}^{T4}, V_{i|k}^{T5}, V_{i|k}^{T6} \\ &\eta_{i|k}^{1:5}, \eta_{i|k}^{1:10}, \eta_{i|k}^{1:15}, \eta_{i|k}^{3:5}, \eta_{i|k}^{3:10}, \eta_{i|k}^{3:15}]^T \end{aligned} \tag{42}$$

$$\begin{aligned} \mathbf{u}_{i|k} = [&q_{2,i|k}^{u}, q_{3,i|k}^{u}, q_{4,i|k}^{u}, q_{6,i|k}^{u}, q_{1,i|k}^{\text{CSO}} \\ &q_{2,i|k}^{\text{CSO}}, q_{3,i|k}^{\text{CSO}}, q_{4,i|k}^{\text{CSO}}, q_{5,i|k}^{\text{CSO}}, q_{6,i|k}^{\text{CSO}}]^T \end{aligned} \tag{43}$$

$$\mathbf{w}_{i|k} = [w_{i|k}^{T1}, w_{i|k}^{T2}, w_{i|k}^{T3}, w_{i|k}^{T4}, w_{i|k}^{T5}, w_{i|k}^{T6}]^T \tag{44}$$

where $\mathbf{x}_{i|k}$ is tank volume V^T and the delayed flows between tanks $\eta^{a:b}$ with a as destination and b the remaining travel time. $\mathbf{u}_{i|k}$ consists of the controlled tank outflows as well as the CSOs, while $\mathbf{w}_{i|k}$ only consists of the external tank inflows.

The uncertainty was chosen to be normally distributed. Therefore, quantile functions of constraints can be written as

$$\begin{aligned} \Phi^{-1}_{g_j(u,w)}\{\gamma\} = &E\{g_j(\mathbf{x}_{i|k}, \mathbf{u}_{i|k}, \mathbf{w}_{i|k})\} \\ &+ \sigma\{g_j(\mathbf{x}_{i|k}, \mathbf{u}_{i|k}, \mathbf{w}_{i|k})\}\Phi^{-1}\{\gamma\} \end{aligned} \tag{45}$$

where $\Phi^{-1}\{\gamma\}$ is a quantile of the standard normal distribution.

C. Constraint Reformulation

As the constraint tightening of T-MPC is similar to CC-MPC's, as shown in Section III-C. The presence of uncertainty in UDS gives T-MPC the same issue with feasibility and CSO definition, as CC-MPC [17]. For CC-MPC, the issues can be addressed through a revision [17], [18], splitting overflow definition from the uncertainty handling. Using a similar approach, we can remove the issues for the T-MPC, through a reformulation of the constraints. Consider the constraints of a tank with controlled output

$$V_{i+1|k} = V_{i|k} + \Delta T (q^{\text{in}}_{i|k} - q^{u}_{i|k} - q^{\text{CSO}}_{i|k}) \quad (46)$$

$$0 \le V_{i|k} + \Delta T (q^{\text{in}}_{i|k} - q^{u}_{i|k} - q^{\text{CSO}}_{i|k}) \le \overline{V} \quad (47)$$

the upper constraint defines CSO $q^{\text{CSO}}_{i|k}$ at the ith prediction.

If we consider volume $V_{i|k}$ and inflow $q^{\text{in}}_{i|k}$ to be uncertain and bounded, the controlled outflow $q^{u}_{i|k}$ and CSO flow $q^{\text{CSO}}_{i|k}$ as optimization variables, the robust constraints become

$$\max(-V_{i|k} - \Delta T q^{\text{in}}_{i|k}) \le -\Delta T (q^{u}_{i|k} + q^{\text{CSO}}_{i|k}) \quad (48)$$

$$\max(V_{i|k} + \Delta T q^{\text{in}}_{i|k}) - \Delta T (q^{u}_{i|k} + q^{\text{CSO}}_{i|k}) \le \overline{V} \quad (49)$$

for the direct application of T-MPC. For the revised T-MPC, (49) is divided into a nominal and worst case constraint

$$\tilde{V}_{i|k} + \Delta T \tilde{q}^{\text{in}}_{i|k} - \Delta T (q^{u}_{i|k} + q^{\text{CSO}}_{i|k}) \le \overline{V} \quad (50)$$

$$\max(V_{i|k} + \Delta T q^{\text{in}}_{i|k}) - \Delta T q^{u}_{i|k} - c_{i|k} \le \overline{V}. \quad (51)$$

The CSO $q^{\text{CSO}}_{i|k}$ is now defined by the constraint (50) based on the nominal constraint, while (51) formulates the robustness of avoiding CSO. The unbound slack variable c is introduced into (51) to guarantee feasibility when CSO cannot be avoided ($q^{\text{CSO}}_{i|k} > 0$). For the lower constraint in (48), the revised version can be obtained by introducing a bounded slack variable s for the feasibility issue

$$\max(-V_{i|k} - \Delta T q^{\text{in}}_{i|k}) - s_{i|k} \le -\Delta T (q^{u}_{i|k} + q^{\text{CSO}}_{i|k}) \quad (52)$$

$$s_{i|k} \le \|\Delta V_{i|k} + \Delta T \Delta q^{\text{in}}_{i|k} k\|_1 \quad (53)$$

$$0 \le s_{i|k}, c_{i|k} \quad (54)$$

the upper bound on the slack variable s is set as equal to the constriction as discussed in (32). The expected value in (50) is defined as the mean of the bounds of the uncertainty.

D. Cost Formulation

The cost in the MPC design is the quadratic-linear cost in (55). It contains a weighted sum of quadratic cost on the change of control flow, and linear costs on the accumulated CSO volume $\mathbf{V}^{\text{CSO}}_{k}$, and the objectives $\mathbf{z}_k$; maximum flow to WWTP and minimum CSO flow. The outflow term in T-MPC and CC-MPC is formulated as the maximum and the expectation, respectively,

$$J = \min_{\mathbf{q}^{u}, \mathbf{q}^{\text{CSO}}} \Sigma_{j=0}^{N} \|\Delta \mathbf{q}^{u}_{j|k}\|^2_R + \mathbf{Q}^T \mathbf{z}_{j|k} + \mathbf{W}^T \mathbf{V}^{\text{CSO}}_{j|k} \quad (55)$$

$$\mathbf{z}_{j|k} = [q^{\text{out},T1}_{j|k}, \Sigma_{i=1}^{6} \mathbf{q}^{\text{CSO}}_{i,j|k}] \quad (56)$$

$$\mathbf{V}^{\text{CSO}}_{j|k} = \Sigma_{i=0}^{j} \Delta T \mathbf{q}^{\text{CSO}}_{i|k}. \quad (57)$$

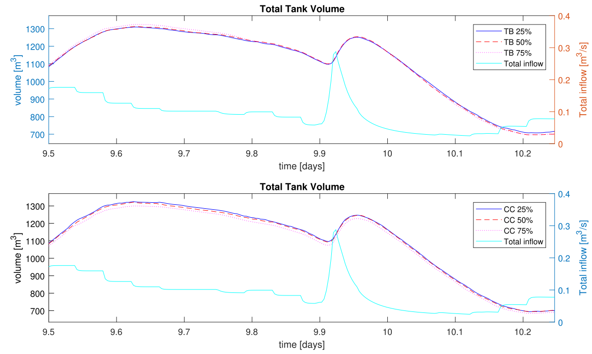

Fig. 3. Volume of T-MPC and CC-MPC with uncertainty bounds 25%–75%.

For the T-MPC and CC-MPC the slack cost term $\mathbf{W}_c^T \mathbf{c} + \mathbf{W}_s^T \mathbf{s}$ is added. The weights of the terms are -1 for the WWTP outflow, 2 for CSO flow, and 0.01 for the control change flow, while weights of the CSO volume are differentiated across tanks, tank 1 is 1000, tanks 2–5 is 5000, and tank 6 is 10 000, given importance to avoid CSO to the creek over the river. The weights for the added slack terms are 10.

V. Performance Comparison and Results Discussion

Simulations were performed using a dataset of rainfall for one year. A prediction horizon of 100 min was chosen with a sampling time of 5 min. The horizon was chosen based on the forecast horizons used by utility companies, also covering input–output period of the system dynamics, ∼60 min, see Fig. 2. In the simulations, CC-MPC is used with a confidence level γ of 90% for all probabilistic constraints, for a fair comparison. MPC with no uncertainty consideration is used as a baseline.

In each simulation, a single parameter was changed to compare the sensitivity between controllers toward the given parameter. The parameters considered are bounds on the uncertainty, scaling bias, and offset bias of the expected disturbance. For each parameter, a base value was chosen (50% for bound uncertainty, 0% for scaling bias, and 0 for offset bias).

A. Uncertainty Bound

The uncertainty in the inflow disturbance q is defined by (58), where the disturbance is assumed to be non-negative and below three standard deviations σ above the expected inflow

$$\text{bound} = [0, \mathbb{E}\{q\} + 3\sigma]. \quad (58)$$

In the simulations, the standard deviation was varied so that the upper bound would correspond to 25%, 50%, and 75% above the expected value. The results for each of the controller types with three sizes of uncertainty bounds can be observed in Table I for CSO and treated wastewater volume.

From these comparisons, it can be observed that CC-MPC performs slightly better than T-MPC in total CSO volume. Moreover, we can conclude that T-MPC performs worse as the uncertainty bound increases, while CC-MPC works better with an increase in uncertainty bounds. Fig. 3 also supports this conclusion (for a clear view, only around day 10 are shown).

The difference in how the MPC approaches are affected by the increase in the uncertainty bound is consistent and can be

TABLE I

Overflow and Treated Wastewater Results of SWMM Simulations With MPC, CC-MPC, and T-MPC With Uncertainty Bound of 25%–75%

CSO Recipient	MPC	CC-MPC 25%	T-MPC 25%	CC-MPC 50%	T-MPC 50%	CC-MPC 75%	T-MPC 75%
River $[m^3]$	183754	183879 (0.0680%)	181174 (-1.4041%)	183778 (0.0131%)	183509 (-0.1333%)	183412 (-0.1861%)	185473 (0.9355)
Creek $[m^3]$	45996	45984 (-0.0261%)	49630 (7.9007%)	45990 (-0.0130%)	47778 (3.8742%)	45718 (-0.6044%)	46532 (1.1653%)
Total $[m^3]$	229750	229864 (0.0496%)	230804 (0.4588%)	229768 (0.0078%)	231287 (0.6690%)	229130 (-0.2699%)	232005 (0.9815%)
WWTP	**MPC**	**CC-MPC 25%**	**T-MPC 25%**	**CC-MPC 50%**	**T-MPC 50%**	**CC-MPC 75%**	**T-MPC 75%**
Vol. $[m^3]$	3772057	3772086 (0.0008%)	3771026 (-0.0273%)	3772159 (0.0027%)	3770439 (-0.0429%)	3772676 (0.0164%)	3769809 (-0.0596%)

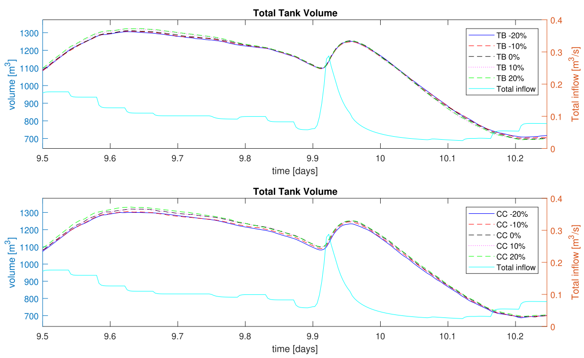

Fig. 4. Volume in tanks of T-MPC and CC-MPC with different scales.

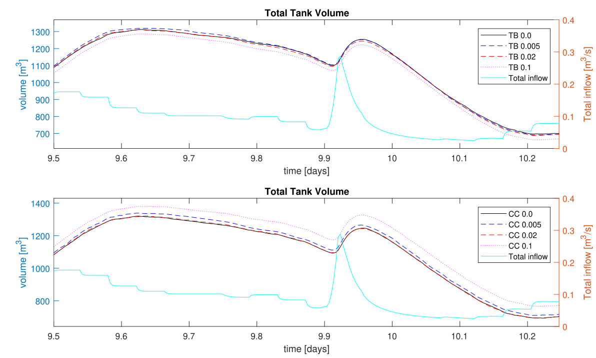

Fig. 5. Tank volumes of T-MPC and CC-MPC with different offsets.

explained by their formulation; while both become more strict or conservative, the T-MPC expects more inflow (higher bound mean), resulting in a bottleneck with increased upstream local volumes (creek), and an increased CSO in the entire system. For the treated wastewater, we can see that both controllers are in general indifferent to the change of the uncertainty bound.

B. Scaled Bias

The scaling bias a is defined in (59), with negative scaling indicating underestimation of the actual disturbance, and positive for overestimation of the actual disturbance

$$\mathbb{E}\{q\} = (1+a)q^{\text{actual}}. \tag{59}$$

The results of CSO and amount of treated wastewater can be seen in Table II, for different scaling biases: 0%, ±10%, and ±20%. It is clear that for both T-MPC and CC-MPC, CSO performance is deteriorating as the scaling bias increases, though T-MPC is less sensitive. It can also be seen that T-MPC performs slightly worse than both the MPC (no uncertainty) and CC-MPC. For T-MPC, we again observe a deterioration of the CSO distribution, which is not seen for CC-MPC.

Fig. 4 illustrates the total tank volume evolution of the MPC approaches. We observe that MPCs with a 20% bias have larger tank volume peaks, which indicates more CSO may occur. There is a slight trend showing that the increase of scaled bias slightly increases the tank volumes.

When considering treated wastewater, improvements and deteriorations become close to negligible for both controllers. With the caveat that both MPC approaches perform worse as the bias increases toward positive.

C. Offset Bias

Offset b [as in (60)] shifts expected disturbance away from actual disturbance. The following offsets were used: 0, 0.25, 1, and 5 times the average inflow disturbance

$$\mathbb{E}\{q\} = q^{\text{actual}} + b. \tag{60}$$

In Table III, we can observe the results. For treated wastewater, the T-MPC is less sensitive to increases in offset biases than CC-MPC. It can also be observed that for lower offsets, the deviation from the results of the perfect MPC is negligible, but that of the CC-MPC has less deviation.

For the results of CSO volume, we observe that the sensitivity to an offset increase is significantly lower for T-MPC than for CC-MPC. While the performance of T-MPC is slightly worse at lower offsets, the CC-MPC significantly deteriorates at higher offsets, where T-MPC is less affected. For both cases, the distribution of CSO improves as the offset increases, but with deteriorating performances as a result. For the T-MPC, the CSO distribution through the system is in general performing significantly worse than for the CC-MPC.

In Fig. 5, the performance of T-MPC and CC-MPC under different offsets is shown. As higher volumes indicate a larger chance of future CSOs, we can conclude that the CC-MPC with 0.1 offsets performs worse than the other CC-MPCs, as the tank volume is higher; as observed in Table III.

D. Computational Time

By considering the maximum and mean computation time for a single optimization, the perfect MPC has a mean computation of approximately 0.061 s, with a maximal time of around 0.247 s. The mean time for T-MPC and CC-MPC are comparable, with only slight differences; generally around 0.11 and 0.10 s, respectively. Both are around twice as slow on average as the perfect MPC. Both MPCs are generally consistent in their mean computation time, regardless of the scenario. The general maximum time for T-MPC and CC-MPC, 0.30 and 0.28 s, is comparable, consistent across scenarios, and only slightly higher than the perfect MPC.

VI. Discussion—Pros and Cons

Despite the shown similarities between the two methods, the approach to uncertainty gives different pros and cons.

TABLE II

OVERFLOW AND TREATED WASTEWATER RESULTS WITH MPC, CC-MPC, AND T-MPC WITH SCALED UNCERTAINTY BIAS FROM −20% TO 20%

Recipient	MPC	Type	-20%	-10%	0%	10%	20%
River $[m^3]$	183754	CC-MPC	182242 (-0.8228%)	182623 (-0.6155%)	183778 (0.0131%)	185094 (0.7292%)	187129 (1.8367%)
		T-MPC	181526 (-1.2125%)	182301 (-0.7907%)	183509 (-0.1333%)	184423 (0.3641%)	185076 (0.7194%)
Creek $[m^3]$	45996	CC-MPC	47126 (2.4567%)	46341 (0.7501%)	45990 (-0.0130%)	45815 (-0.3935%)	45880 (-0.2522%)
		T-MPC	49177 (6.9158%)	48395 (5.2157%)	47778 (3.8742%)	47144 (2.4959%)	46799 (1.7458%)
Total $[m^3]$	229750	CC-MPC	229368 (-0.1663%)	228964 (-0.3421%)	229768 (0.0078%)	230909 (0.5045%)	233008 (1.4181%)
		T-MPC	230704 (0.4152%)	230696 (0.4118%)	231287 (0.6690%)	231567 (0.7909%)	231875 (0.9249%)
	MPC	**Type**	**-20%**	**-10%**	**0%**	**10%**	**20%**
WWTP Vol. $[m^3]$	3772057	CC-MPC	3772166 (0.0029%)	3772992 (0.0248%)	3772159 (0.0027%)	3770672 (-0.0367%)	3768942 (-0.0826%)
		T-MPC	3771113 (-0.0250%)	3770657 (-0.0371%)	3770439 (-0.0429%)	3770220 (-0.0487%)	3769903 (-0.0571%)

TABLE III

OVERFLOW AND TREATED WASTEWATER RESULTS WITH MPC, CC-MPC, AND T-MPC WITH OFFSET UNCERTAINTY BIAS

Recipient	MPC	Type	0	0.005	0.02	0.1
River $[m^3]$	183754	CC-MPC	183778 (0.0131%)	184536 (0.4256%)	187360 (1.9624%)	222925 (21.3171%)
		T-MPC	183509 (-0.1333%)	183437 (-0.1725%)	184158 (0.2199%)	189244 (2.9877 %)
Creek $[m^3]$	45996	CC-MPC	45990 (-0.0130%)	46005 (0.0196%)	45825 (-0.3718%)	45808 (-0.4087%)
		T-MPC	47778 (3.8742%)	47689 (3.6808%)	47106 (2.4133%)	45653 (-0.7457%)
Total $[m^3]$	229750	CC-MPC	229768 (0.0078%)	230541 (0.3443%)	233185 (1.4951%)	268733 (16.9676%)
		T-MPC	231287 (0.6690%)	231126 (0.5989%)	231264 (0.6590%)	234897 (2.2403%)
	MPC	**Type**	**0**	**0.005**	**0.02**	**0.1**
WWTP Vol. $[m^3]$	3772057	CC-MPC	3772159 (0.0027%)	3771978 (-0.0021%)	3768643 (-0.0905%)	3733651 (-1.0182%)
		T-MPC	3770439 (-0.0429%)	3770306 (-0.0464%)	3770471 (-0.0420%)	3767206 (-0.1286%)

TABLE IV

REQUIREMENTS, PROS, AND CONS OF T-MPC AND CC-MPC METHODS

	Bounded	distribution	Propagation	conservatism	Bias Sensitive	Uncertainty sensitive	UDS Best
T-MPC	required	not required	easier	maxed, $\gamma = 1$	no	yes	specific cases
CC-MPC	optional	any (known)	harder	tunable by γ	yes	no	generally

CC-MPC handles unbounded uncertainties, and has a tunable degree γ of conservatism, but has to know the exact distribution, while T-MPC is nontunable ($\gamma = 1$), with constraints assumed uniform. T-MPC is more conservative than CC-MPC in handling uncertainty, with stricter tightenings of constraints, and higher costs. CC-MPC is, in general, more computationally heavy than T-MPC, given the complexity of propagating distributions over bounds, and computing the constraint quantiles.

Based on the simulations, we conclude that T-MPC works better for achieving a performance that is insensitive to bias uncertainties, while the CC-MPC is more insensitive to the size of the uncertainty bound. If the preference is given to the performance (CSO/treated wastewater), then, in general, the CC-MPC works better except for a few cases of extreme uncertainty. The difference in performance between CC-MPC and T-MPC is usually around 1000 m^3, corresponding to $\sim 0.3\%$ difference with respect to the perfect MPC for CSO performance. The pros and cons are summarized in Table IV.

VII. CONCLUSION

In this brief, a reformulated T-MPC using zonotopes has been presented and successfully applied to address the CSO problem in UDS. The similarities and differences of T-MPC and CC-MPC were compared and discussed; including how the different assumptions on uncertainty affect the constriction of constraints, and the drawbacks of each method. Performance of the revised T-MPC is evaluated on a benchmark UDS, the Astlingen benchmark network, simulated on a Hi-Fi SWMM platform.

The conclusions of the analysis and results are summarized as follows.

1) T-MPC is computationally simpler than CC-MPC, given the complexity of quantile functions, although under certain assumptions CC-MPC can be simpler, e.g., Gaussian.
2) T-MPC is worst case conservative and requires bounded disturbances, while CC-MPC has tunable conservatism and is applicable for unbounded disturbances.
3) CC-MPC assumes distribution is known, while T-MPC assumes bounds to be known. In stochastic terms, T-MPC is equivalent to the assumption of uniform distribution.
4) Constraint constriction of T-MPC and CC-MPC have an inequality relation, where the T-MPC constriction is always stricter than that of CC-MPC.
5) Performance-wise, the simulation results show that CC-MPC in general provides better performance in CSO than T-MPC; CC-MPC is less sensitive to uncertainty size, while T-MPC is less sensitive to bias variations.
6) The performance in treated wastewater of both T-MPC and CC-MPC is generally insensitive to uncertainty.

Considering the MPCs' strengths and weaknesses in handling CSO in UDS, future research directions can be proposed.

1) The performance/formulation of zonotope-based T-MPC with more information, e.g., expectation.
2) Analysis of the CSO-problem with the inclusion of complex distributions, or the scenario-based MPC [35].
3) Defining conditions for standardization tricks for simple computations, as (45) is a fair representation or efficient estimation of propagated distributions for CC-MPC.

REFERENCES

[1] C. Sun et al., "Integrated pollution-based real-time control of sanitation systems," *J. Environ. Manag.*, vol. 269, Sep. 2020, Art. no. 110798.

[2] J. L. Svensen, H. H. Niemann, and N. K. Poulsen, “Model predictive control of overflow in sewer networks: A comparison of two methods,” in *Proc. 4th Conf. Control Fault Tolerant Syst. (SysTol)*, Sep. 2019, pp. 412–417.

[3] C. Sun, J. L. Svensen, M. Borup, V. Puig, G. Cembrano, and L. Vezzaro, “An MPC-enabled SWMM implementation of the Astlingen RTC benchmarking network,” *Water*, vol. 12, no. 4, p. 1034, Apr. 2020.

[4] M. Marinaki and M. Papageorgiou, *Optimal Real-time Control of Sewer Networks* (Advances in Industrial Control). Berlin, Germany: Springer, 2005.

[5] J. M. Grosso, C. Ocampo-Martínez, V. Puig, and B. Joseph, “Chance-constrained model predictive control for drinking water networks,” *J. Process Control*, vol. 24, no. 5, pp. 504–516, May 2014.

[6] M. Nassourou, J. Blesa, and V. Puig, “Robust economic model predictive control based on a zonotope and local feedback controller for energy dispatch in smart-grids considering demand uncertainty,” *Energies*, vol. 13, no. 3, p. 696, Feb. 2020.

[7] J. L. Svensen, “Peak shaving in district heating utilizing adaptive predictive control,” *Energies*, vol. 15, no. 22, p. 8555, Nov. 2022. [Online]. Available: https://www.mdpi.com/1996-1073/15/22/8555

[8] Q. Weiwei, L. Jieyu, H. Xiaoxiang, H. Bing, and L. Gang, “Tube-based active robust MPC for uncertain constrained linear systems with time delays,” *IEEE Access*, vol. 7, pp. 125552–125561, 2019.

[9] J. B. Rawlings, D. Q. Mayne, and M. M. Diehl, *Model Predictive Control: Theory, Computation, and Design*, 2nd ed. Madison, Wiscosin: Nob Hill, Oct. 2017.

[10] P. O. M. Scokaert and J. B. Rawlings, “Stability of model predictive control under perturbations,” in *Proc. IFAC Symp. Nonlinear Control Syst. Design*, Jun. 1995, pp. 19–24.

[11] C. Sun, B. Joseph, G. Cembrano, V. Puig, and J. Meseguer, “Advanced integrated real-time control of combined Urban drainage systems using MPC,” in *Proc. 13th Int. Conf. Hydroinformatic*, 2018, pp. 2033–2041.

[12] C. Sun et al., “Efficient integrated model predictive control of urban drainage systems using simplified conceptual quality models,” in *Proc. 14th IWA/IAHR Int. Conf.*, 2017, pp. 1848–1855.

[13] C. Sun, M. Morley, D. Savic, V. Puig, G. Cembrano, and Z. Zhang, “Combining model predictive control with constraint-satisfaction formulation for the operative pumping control in water networks,” in *Proc. 13th Comput. Control Water Ind. Conf.*, Sep. 2015, pp. 963–972.

[14] C. C. Sun, V. Puig, and G. Cembrano, “Multi-layer model predictive control of regional water networks: Application to the Catalunya case study,” in *Proc. 52nd IEEE Conf. Decis. Control*, Dec. 2013, pp. 7095–7100.

[15] C. Sun, V. Puig, and G. Cembrano, “Two-layer scheduling scheme for pump stations,” in *Proc. IEEE Conf. Control Appl.*, Oct. 2014, pp. 1741–1746.

[16] Z. Sun, L. Dai, K. Liu, Y. Xia, and K. H. Johansson, “Robust MPC for tracking constrained unicycle robots with additive disturbances,” *Automatica*, vol. 90, pp. 172–184, Apr. 2018.

[17] J. L. Svensen, H. H. Niemann, A. K. V. Falk, and N. K. Poulsen, “Chance-constrained model predictive control a reformulated approach suitable for sewer networks,” *Adv. Control Appl., Eng. Ind. Syst.*, vol. 3, no. 4, p. e94, Oct. 2021.

[18] J. L. Svensen, C. Sun, G. Cembrano, and V. Puig, “Chance-constrained stochastic MPC of Astlingen urban drainage benchmark network,” *Control Eng. Pract.*, vol. 115, Oct. 2021, Art. no. 104900.

[19] D. L. Marruedo, T. Alamo, and E. F. Camacho, “Stability analysis of systems with bounded additive uncertainties based on invariant sets: Stability and feasibility of MPC,” in *Proc. Amer. Control Conf.*, 2002, pp. 364–369.

[20] H. Arellano-Garcia and G. Wozny, “Chance constrained water quality management model for reservoir systems: I. Strict monotonicity,” *Comput. Chem. Eng.*, vol. 33, no. 10, pp. 1568–1583, 2009.

[21] A. D. Bonzanini, T. L. M. Santos, and A. Mesbah, “Tube-based stochastic nonlinear model predictive control: A comparative study on constraint tightening,” in *Proc. 12th IFAC Symp. Dyn. Control Process Syst., Including Biosyst.*, vol. 52, Florianopolos, Brazil, Apr. 2019, pp. 598–603.

[22] A. Dhar and B. Datta, “Chance constrained water quality management model for reservoir systems,” *ISH J. Hydraulic Eng.*, vol. 12, no. 3, pp. 39–48, Jan. 2006.

[23] M. Evans, M. Cannon, and B. Kouvaritakis, “Linear stochastic MPC under finitely supported multiplicative uncertainty,” in *Proc. Amer. Control Conf. (ACC)*, Jun. 2012, pp. 442–447.

[24] K. Hariprasad and S. Bhartiya, “A computationally efficient robust tube based MPC for linear switched systems,” *Nonlinear Anal., Hybrid Syst.*, vol. 19, pp. 60–76, Feb. 2016.

[25] B. Kouvaritakis and M. Cannon, *Model Predictive Control: Classical, Robust, and Stochastic* (Advances Textbooks in Control and Signal Processing). Berlin, Germany: Springer, 2016.

[26] D. Limon, T. Alamo, F. Salas, and E. F. Camacho, “Input to state stability of min-max MPC controllers for nonlinear systems with bounded uncertainties,” *Automatica*, vol. 42, no. 5, pp. 797–803, 2006.

[27] L. Magni, G. De Nicolao, R. Scattolini, and F. Allgöwer, “Robust model predictive control for nonlinear discrete-time systems,” *Int. J. Robust Nonlinear Control*, vol. 13, nos. 3–4, pp. 229–246, Mar. 2003.

[28] A. Mesbah, “Stochastic model predictive control: An overview and perspectives for future research,” *IEEE Control Syst. Mag.*, vol. 36, no. 6, pp. 30–44, Dec. 2016.

[29] Z. Wan and M. V. Kothare, “Robust output feedback model predictive control using off-line linear matrix inequalities,” *J. Process Control*, vol. 12, no. 7, pp. 763–774, Oct. 2002.

[30] V. Raghuraman and J. P. Koeln, “Tube-based robust MPC with adjustable uncertainty sets using zonotopes,” in *Proc. Amer. Control Conf. (ACC)*, May 2021, pp. 462–469.

[31] M. C. Campi, S. Garatti, and M. Prandini, “The scenario approach for systems and control design,” *Annu. Rev. Control*, vol. 33, no. 2, pp. 149–157, Dec. 2009.

[32] A. T. Schwarm and M. Nikolaou, “Chance-constrained model predictive control,” *AIChE J.*, vol. 45, no. 8, pp. 1743–1748, Aug. 1999.

[33] E. González, J. Sanchis, S. García-Nieto, and J. Salcedo, “A comparative study of stochastic model predictive controllers,” *Electronics*, vol. 9, no. 12, p. 2078, Dec. 2020.

[34] M. Farina, L. Giulioni, and R. Scattolini, “Stochastic linear model predictive control with chance constraints—A review,” *J. Process Control*, vol. 44, pp. 53–67, Aug. 2016.

[35] H. A. Nasir, M. Cantoni, Y. Li, and E. Weyer, “Stochastic model predictive control based reference planning for automated open-water channels,” *IEEE Trans. Control Syst. Technol.*, vol. 29, no. 2, pp. 607–619, Mar. 2021.

[36] J. M. Grosso, P. Velarde, C. Ocampo-Martinez, J. M. Maestre, and V. Puig, “Stochastic model predictive control approaches applied to drinking water networks,” *Optim. Control Appl. Methods*, vol. 38, no. 4, pp. 541–558, Jul. 2017.

[37] M. S. Gelormino and N. L. Ricker, “Model-predictive control of a combined sewer system,” *Int. J. Control*, vol. 59, no. 3, pp. 793–816, Mar. 1994.

[38] V. P. Singh, *Hydrologic Systems: Rainfall-Runoff Modeling*, vol. 1. Upper Saddle River, NJ, USA: Prentice-Hall, 1988.

[39] C. Ocampo-Martinez, *Model Predictive Control of Wastewater Systems* (Advances in Industrial Control). Berlin, Germany: Springer, 2010.

[40] M. Beck and S. Robins, *Computing the Continous Discretely—Integer-Point Enumeration in Polyhedra*. Berlin, Germany: Springer, Oct. 2015, ch. 9, pp. 167–182.

[41] L. Hewing, K. P. Wabersich, and M. N. Zeilinger, “Recursively feasible stochastic model predictive control using indirect feedback,” *Automatica*, vol. 119, Sep. 2020, Art. no. 109095.

[42] A. Benavoli and D. Piga, “A probabilistic interpretation of set-membership filtering: Application to polynomial systems through polytopic bounding,” *Automatica*, vol. 70, pp. 158–172, Aug. 2016.

[43] M. Schutze, M. Lange, M. Pabst, and U. Haas, “Astlingen—A benchmark for real time control (RTC),” *Water Sci. Technol.*, vol. 2017, no. 2, pp. 552–560, May 2018.

[44] R. Halvgaard and A. K. V. Falk, “Water system overflow modeling for model predictive control,” in *Proc. 12th IWA Specialised Conf. Instrum., Control Autom.*, Jun. 2017, pp. 1–4.